Theoretical analysis of ridge gratings for long-range surface plasmon polaritons

Thomas Søndergaard,[1,2,*] Sergey I. Bozhevolnyi,[1] and Alexandra Boltasseva[3]
[1]*Department of Physics and Nanotechnology, Aalborg University, Skjernvej 4, DK-9220, Aalborg Øst, Denmark*
[2]*Department of Physics, University of Southern Denmark, Campusvej 55, DK-5230 Odense M, Denmark*
[3]*COM, Technical University of Denmark, Bldg. 345v, DK-2800 Kongens Lyngby, Denmark*
(Received 1 July 2005; revised manuscript received 6 December 2005; published 23 January 2006)

Optical properties of ridge gratings for long-range surface plasmon polaritons (LRSPPs) are analyzed theoretically in a two-dimensional configuration via the Lippmann-Schwinger integral equation method. LRSPPs being supported by a thin planar gold film embedded in dielectric are considered to be scattered by an array of equidistant gold ridges on each side of the film designed for in-plane Bragg scattering of LRSPPs at the wavelength ~1550 nm. Out-of-plane scattering (OUPS), LRSPP transmission, reflection, and absorption are investigated with respect to the wavelength, the height of the ridges, and the length of the grating. Particular attention is paid to the fraction of the LRSPP power lost due to the OUPS. We find an asymmetry in the OUPS spectra in the vicinity of the band gap and relate this asymmetry to that observed in the transmission spectra. It is found that in order to maximize a reflection peak it is preferable to use longer gratings with smaller ridges compared to gratings with larger ridges, because the former result in a smaller OUPS from the grating facets than the latter. The theoretical analysis and its conclusions are supported with experimental results on the LRSPP reflection and transmission by ridge gratings. For comparison, a few calculations are also presented for surface plasmon polariton (SPP) scattering by ridge gratings, a configuration which corresponds to the LRSPP case with a very thick film. We found that, in this case, it is less attractive to use long gratings due to higher propagation loss and stronger confinement of SPPs in comparison with LRSPPs.

DOI: 10.1103/PhysRevB.73.045320 PACS number(s): 42.70.Qs, 71.36.+c, 02.60.−x, 02.70.−c

I. INTRODUCTION

Surface plasmon polaritons (SPPs) are electromagnetic waves that propagate along and are bound to metal-dielectric interfaces.[1] Metal-dielectric interfaces represent an interesting alternative to dielectric waveguides for planar optical components. However, due to the requirement of low loss for optical devices, in particular for telecommunication, it is of interest to reduce the appreciable propagation loss of SPP waves by replacing the metal-dielectric interface with a thin metal film[2,3] or a thin metal stripe[4–6] embedded in a dielectric. The thin metal films and stripes may support guided waves with a much lower propagation loss compared to SPP waves, and these waves are therefore referred to as long-range surface plasmon polaritons (LRSPPs). The cost of achieving the low propagation loss is that LRSPPs are more loosely bound than SPPs, which results in less absorption by the metal.

Microstructuring of planar metal surfaces has been pursued experimentally[7–18] and theoretically[19–28] by a number of researchers with the idea that such structures can be used to manipulate and control the propagation of light in the plane. This includes using a periodic surface microstructuring of metal interfaces and films to create a structure exhibiting a band gap for (LR)SPP waves, i.e., a wavelength interval where propagation of (LR)SPPs in the structure is inhibited. Such microstructured metal films and metal-dielectric interfaces have been referred to as (LR)SPP band gap (BG) structures. This research was largely inspired and influenced by the progress and ideas in the field of planar dielectric photonic crystal structures.[29–31] There exist, however, important differences between these configurations.

A surface microstructure will cause not only the in-plane radiation scattering, i.e., the (LR)SPP-to-(LR)SPP scattering. Part of the (LR)SPP power will be lost due to scattering into electromagnetic waves propagating away from the surface plane. Important issues for such planar (LR)SPP-based microstructures are then related to the out-of-plane scattering (OUPS) efficiency and the influence of OUPS on such characteristics as reflection and transmission of surface waves, especially for BG structures. These are the issues that will be addressed in the present paper concentrating on ridge gratings for LRSPPs. Dielectric grating structures resembling the metallic gratings considered in this paper have been studied in Refs. 32 and 33.

The paper is organized as follows. In Sec. II, the considered ridge gratings for LRSPPs are described, and the numerical method that we use to model the optical and plasmonic properties of the gratings is presented. Numerical results obtained for various LRSPP gratings are shown and discussed in Sec. III. Corresponding experimental measurements of LRSPP reflection and transmission are also presented in this section and compared with our simulations verifying the theoretical approach used and supporting the conclusions reached. In Sec. IV, for comparison, a few calculations are presented for SPP gratings corresponding to using a very thick gold film. The results obtained and the overall conclusions are summarized in Sec. V.

II. LRSPP GRATINGS AND NUMERICAL METHOD

The configuration of LRSPP gratings considered in this paper is illustrated in Fig. 1. The grating consists of a thin gold film of thickness d, and on each side of the film is placed an array of gold ridges of height h, width W, and spacing Λ. The gold film and ridges are surrounded by a

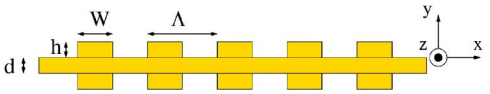

FIG. 1. (Color online) Schematic of a long-range surface plasmon polariton grating. The position $y=0$ corresponds to the upper surface of the thin gold film of thickness d.

polymer with refractive index 1.543. We will use a two-dimensional (2D) model where the grating structure and the electromagnetic fields are treated as being invariant along the z axis, and propagation of electromagnetic waves occurs in the xy plane only. The thin gold film works as a waveguide for two types of waves, namely LRSPPs with a relatively small propagation loss, and short-range surface plasmon polaritons (SRSPPs) with a very large propagation loss. For both LRSPPs and SRSPPs the propagation loss is due to absorption by the gold. The two types of waves have different symmetry across the center of the metal film, and the reason for placing ridges on both sides of the gold film is that then we avoid scattering from LRSPPs into SRSPPs for symmetry reasons. In the remainder of the paper we shall therefore not be concerned with SRSPP waves. Throughout the paper we will use the ridge width $W=230$ nm and the period $\Lambda=500$ nm, where the latter was chosen to give reflection of LRSPPs for wavelengths around 1550 nm. For LRSPP gratings we will use $d=15$ nm, and ridge heights h in the range 10–30 nm.

We are interested in a situation where a LRSPP wave is propagating along the metal film from the left-hand side (along the positive x axis in Fig. 1). As the wave is incident on the region with the ridges, i.e., the grating, there will be reflection into backwards traveling LRSPP waves, transmission through the grating into LRSPP waves, and losses related to out-of-plane scattering and absorption by the gold ridges (and gold film). These optical properties, reflection, transmission, out-of-plane scattering (OUPS), and absorption can be analyzed theoretically via the Lippmann-Schwinger integral equation

$$\mathbf{E}(\mathbf{r}) = \mathbf{E}_0(\mathbf{r}) + \int \mathbf{G}(\mathbf{r},\mathbf{r}')k_0^2(\epsilon(\mathbf{r}') - \epsilon_{ref}(\mathbf{r}')) \cdot \mathbf{E}(\mathbf{r}')d^2r'. \tag{1}$$

In Eq. (1) $\mathbf{E}_0$ is the electric field of the incident LRSPP wave propagating along the thin metal film. $\mathbf{E}_0$ is a field solution in the case when there are no ridges. The incident field used in the numerical calculation is given by the expressions

$$\mathbf{E}_0(\mathbf{r}) = E_0 e^{i\kappa_x x} e^{i\kappa_y y}\left(\hat{y} - \hat{x}\frac{\kappa_y}{\kappa_x}\right), \quad y > 0, \tag{2}$$

$$\mathbf{E}_0(\mathbf{r}) = E_0 e^{i\kappa_x x} A\left(\left[\hat{y} - \hat{x}\frac{\kappa_{y2}}{\kappa_x}\right] e^{i\kappa_{y2} y} + \left[\hat{y} + \hat{x}\frac{\kappa_{y2}}{\kappa_x}\right] e^{-i\kappa_{y2}(y+d)}\right), \quad -d < y < 0, \tag{3}$$

$$\mathbf{E}_0(\mathbf{r}) = E_0 e^{i\kappa_x x} e^{-i\kappa_y (y+d)}\left(\hat{y} + \hat{x}\frac{\kappa_y}{\kappa_x}\right), \quad y < -d. \tag{4}$$

The wave vector components κ_x, κ_y, and κ_{y2} must satisfy $\kappa_x^2+\kappa_y^2=k_0^2\epsilon_{BCB}$, $\kappa_x^2+\kappa_{y2}^2=k_0^2\epsilon_{Au}$, where ϵ_{BCB} is the relative dielectric constant of the background polymer material benzocyclo-butene, and ϵ_{Au} is the relative dielectric constant of gold,[35] and $A=\kappa_y/\{\kappa_{y2}[1-\exp(-i\kappa_{y2}d)]\}$. The sign of κ_y is chosen such that the field magnitude decays exponentially away from the metal film. The LRSPP mode index κ_x/k_0 is obtained by solving the dispersion equation for LRSPP waves (resulting from the boundary conditions at the film interfaces) given in, e.g., Ref. 3. $\hat{x}$ and $\hat{y}$ are unit vectors along the direction of the x axis and y axis, respectively.

As a result of scattering and absorption by the ridges, the electric field is modified so that the resulting total field is $\mathbf{E}$. ϵ_{ref} is the dielectric constant of the thin metal film without the ridges, and ϵ is the dielectric constant of the total structure including the ridges. The difference term $(\epsilon-\epsilon_{ref})$ is the modification made to the thin film structure by the presence of the ridges. k_0 is the free-space wave number, $\mathbf{G}$ is the 2D dyadic Green's tensor for the thin-film structure without the ridges, and $\mathbf{r},\mathbf{r}'$ are position vectors. The Green's tensor was obtained via Sommerfeld integrals similar to Ref. 34. $\mathbf{G}$ is equivalent to the electric field generated in the thin film structure by a line source. Note that $\mathbf{G}$ also depends on the wavelength considered, the thickness d, and the (wavelength-dependent) dielectric constants of the materials involved in the thin-film structure. The dielectric constant for gold vs wavelength is given in Ref. 35. Reflection and transmission are evaluated from the scattered field and total field, respectively, at positions close to the film surface but far from the grating, so that the field related to out-of-plane propagating waves is negligible. The out-of-plane scattering is calculated by integrating the angular spectrum of scattered light in the far field zone. The method is very general and can be applied to many other kinds of ridge shapes, e.g., ridges with rounded corners, triangles, etc. The choice of ridge shape used here was chosen to make the structures comparable to structures that have been experimentally realized.[14,15]

III. ANALYSIS OF THE OPTICAL PROPERTIES OF LRSPP GRATINGS

Figure 2 shows a calculation of the optical properties reflection, transmission, and out-of-plane scattering, for three LRSPP gratings. The three gratings all have the same ridge height $h=10$ nm but different lengths given in number of ridges $N=80$, 160, and 320. The figure shows the fraction of the power of the incident beam that goes into the reflected LRSPP wave (thin solid line: R), the transmitted LRSPP wave (thin dashed line: T), and the fraction going into out-of-plane scattering (thin dotted line: OUPS). We have also found it useful to plot the total power going into the in-plane waves (thick solid line: $R+T$), and the sum of reflection, transmission, and out-of-plane scattering (thick dashed line: $R+T+$OUPS). From the latter curve we may deduce the loss due to absorption by the gold which is $1-(R+T+\text{OUPS})$. In the top of Fig. 1 we consider a rather short grating with only

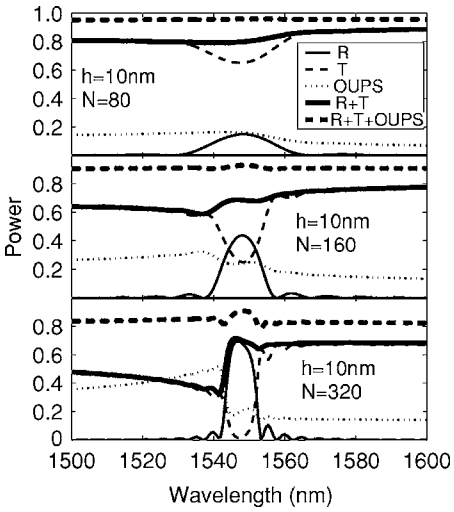

FIG. 2. Reflection (R), transmission (T), and out-of-plane scattering (OUPS) for LRSPP gratings with a 15 nm gold film and $N=80$, 160, and 320 gold ridges of height $h=10$ nm, width $W=230$ nm, and spacing $\Lambda=500$ nm. The gold film and ridges are surrounded by a polymer with refractive index 1.543.

80 periods. A reflection peak is observed for wavelengths around 1550 nm, and a corresponding dip in transmission is seen for the same wavelength. The wavelength range of the reflection peak/transmission dip is the band-gap range of wavelengths for the grating. We notice that for wavelengths longer than the band gap, the transmission is slightly higher than is the case for wavelengths shorter than the band-gap range of wavelengths. The out-of-plane scattering is, however, behaving opposite, as here OUPS is larger for wavelengths shorter than the band gap compared to OUPS for wavelengths longer than the band gap. In fact we may attribute the asymmetry in the transmission across the band gap to the behavior of the out-of-plane scattering. Notice that the absorption loss ($1-R-T-$OUPS) only amounts to a few percent and is not very sensitive to the wavelength. In the middle part of Fig. 2 we have shown the result for twice the grating length ($N=160$ ridges). Now the reflection peak and transmission dip are more pronounced, and the out-of-plane scattering has increased for all wavelengths, but the increase is larger for wavelengths shorter than the band gap, and consequently the asymmetry in transmission across the band gap is larger. Notice that there is a very small peak in $R+T+$OUPS for wavelengths in the band-gap region, meaning that the absorption loss is smaller for wavelengths in the band gap. This is in accordance with the fact that when propagation of light (or LRSPPs) in the grating is inhibited the overlap between the ridges and the field will be smaller, and this leads to less absorption by the gold. If we once more double the number of ridges to $N=320$ we get the result at the bottom of Fig. 2. Notice that compared to $N=160$ the OUPS has only increased for wavelengths shorter than the band gap. For wavelengths longer than the band gap the OUPS has not changed much. In fact, for wavelengths longer than but close to the bandgap the OUPS has even decreased. Notice also that the decrease in absorption loss for wavelengths in the band gap becomes more pronounced as we

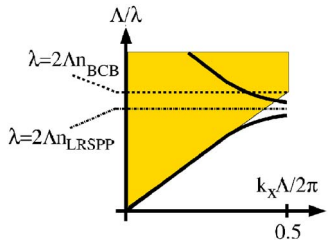

FIG. 3. (Color online) Schematic of the bandstructure for a fully periodic LRSPP grating (number of ridges $N=\infty$.) The shaded continuum corresponds to out-of-plane propagating waves, i.e., combinations of frequencies (Λ/λ) and in-plane Bloch wave numbers (k_x) that are allowed in the polymer material in the absence of the metallic structure. The solid line below the continuum represents a Bloch mode bound to and propagating along the grating structure. The part of the solid line inside the shaded continuum should be interpreted as a resonance due to leakage of light into out-of-plane propagating waves.

increase the length of the grating. For the longer gratings there will for all wavelengths be a contribution to OUPS related to the facets of the grating, or coupling in and out of the grating.

For a fully periodic structure, i.e., a grating with number of ridges $N=\infty$, the field can be expanded in Bloch modes of the form $\mathbf{E}(\mathbf{r})=\mathbf{U}_{k_x}(\mathbf{r})e^{ik_x x}$, where $\mathbf{U}_{k_x}(\mathbf{r})$ is a periodic function with the same periodicity Λ as the grating structure. If we ignore the absorption by the metal, the relationship between the Bloch wave number k_x and the normalized frequency Λ/λ (λ is the wavelength) can be illustrated with the schematic in Fig. 3. The shaded continuum corresponds to the combinations of Bloch wave number and frequency that are allowed in the polymer material in the absence of the metal structure, i.e., the shaded continuum represents the out-of-plane propagating waves. The discrete band shown below the continuum represents a Bloch mode bound to and propagating along the metal structure. In this case there is no leakage of light into out-of-plane propagating waves. However, the part of a discrete solid line located inside the shaded continuum should be interpreted as a resonance. This is not a mode being truly bound to the metal structure. In this case light will be coupled to out-of-plane propagating waves. Notice that the bands in Fig. 3 have been folded into the first Brillouin zone. A consequence of this folding of bands is that for wavelengths shorter than $2\Lambda n_{\mathrm{BCB}}=1543$ nm there are no truly bound modes available, only resonances. On the other hand, for wavelengths slightly larger than $2\Lambda n_{\mathrm{BCB}}$ there will be the discrete band of truly bound modes with no leakage of light into out-of-plane propagating waves. For a very weak grating the band gap will be located around the wavelength $\lambda=2\Lambda n_{\mathrm{LRSPP}}$, where n_{LRSPP} is the mode index (κ_x/k_0) of the LRSPP wave existing in the absence of the ridges. The index n_{LRSPP} can be calculated using, e.g., the method of Ref. 3, by using the present gold film thickness (15 nm), the gold dielectric constant tabulated in Ref. 35, and the dielectric constant of the polymer, which for the wavelengths 1500 nm to 1600 nm results in the real part of the mode index being in the range from 1.5448–1.5446, resulting in a band gap around $\lambda=1545$ nm. As the strength of the grating increases

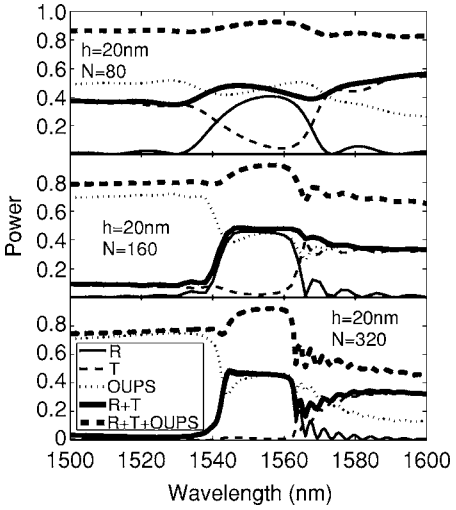

FIG. 4. Reflection (R), transmission (T), and out-of-plane scattering (OUPS) for LRSPP gratings with a 15 nm gold film and $N=80$, 160, and 320 gold ridges of height $h=20$ nm, width $W=230$ nm, and spacing $\Lambda=500$ nm. The gold film and ridges are surrounded by a polymer with refractive index 1.543.

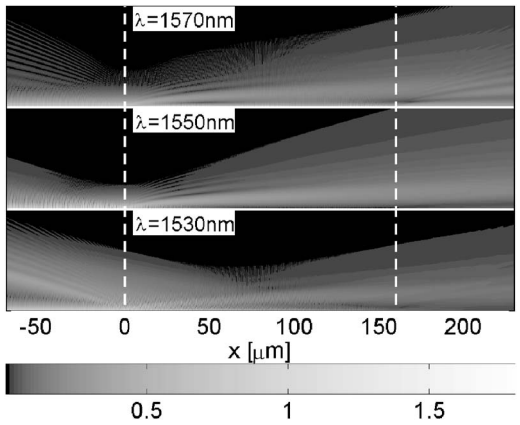

FIG. 5. Electric field magnitude versus height above and position along a LRSPP grating with 320 ridges of height 20 nm. The field magnitude is shown for three wavelengths, $\lambda=1530$ nm ($<$bandgap), $\lambda=1550$ nm (in bandgap), and $\lambda=1570$ nm ($>$bandgap).

beyond the limit of very weak gratings the short-wavelength band-gap edge will remain close to $\lambda=1545$ nm, whereas the long-wavelength band-gap edge shifts to longer wavelengths. These considerations explain that there will be efficient out-of-plane scattering in Fig. 2 for $\lambda<1543$ nm, at least, and that the out-of-plane scattering for these wavelengths increases with the length of the grating. We can also understand that for wavelengths slightly larger than 1543 nm out-of-plane scattering can be small due to the existence of leakage-free Bloch waves of the fully periodic grating structure. For structures with real dielectric constants (no ohmic losses) it is possible to calculate the density-of-states (DOS) of the leaky modes of a grating of infinite length,[36] and from the DOS estimate their lifetime. In our case the situation is more complex due to out-of-plane scattering resulting from coupling light into and out from the grating, and due to ohmic losses.

Figure 4 shows a similar calculation for gratings with ridge height $h=20$ nm. If we compare the peak reflection for different lengths of the grating with the $h=10$ nm case we notice that the reflection is higher for $N=80$ ridges, approximately the same for $N=160$, and significantly smaller for $N=320$. Naturally for very short gratings it helps to increase the size of the ridges. However, the OUPS loss from the facets related to coupling light in and out of the grating will be larger in the case $h=20$ nm, and this loss will ultimately limit the maximum reflection that can be achieved. For $h=20$ nm it is seen that the peak reflection does not change much when doubling the grating length from $N=160$ to $N=320$. For $N=320$ and wavelengths shorter than the band gap practically all light is lost to either absorption or OUPS. We should also notice for $N=160$, 320 ($h=20$ nm) that it is no longer easy to identify a single clear transmission dip revealing the precise location of the band gap, whereas the band gap is easily identified from the reflection peak. A similar effect has been seen for two-dimensional surface plasmon polariton gratings.[24] For wavelengths longer than the band gap the OUPS is here significantly smaller for $N=320$ than for $N=160$. In this case there is a significant influence from the absorption of the light, which results in less light reaching the other end of the grating, which consequently results in less OUPS from the second facet.

Figure 5 shows field magnitude images for a LRSPP grating with ridge height $h=20$ nm and $N=320$ ridges. The field magnitude is shown for a wavelength shorter than the band gap (1530 nm), a wavelength in the band gap (1550 nm), and a wavelength longer than the band gap (1570 nm). For each of the three parts of the figure, the x axis (first axis) is the position along the grating, and the y axis (second axis) is the height above the grating starting from $y=300$ nm above the gold film and going up to $y=60$ μm above the film. The white dashed lines indicate beginning and end of the grating on the film surface. In all cases the incident LRSPP is propagating along the positive x axis, and from the figure for the wavelength $\lambda=1570$ nm we notice that most of the out-of-plane scattering originates from the first facet of the grating at $x=0$. It is possible to see that some OUPS also occurs at the second grating facet ($x=160$ μm) although it is a weak effect. For the wavelength in the band gap ($\lambda=1550$ nm) it is seen from the figure that practically all the out-of-plane scattering originates from the region around the first facet. No scattering is observed to originate from the second facet. The situation changes, however, for the case of the wavelength shorter than the band gap ($\lambda=1530$ nm). Here the OUPS no longer originates mainly from the first facet. Instead it originates mainly from the interior of the grating region. Note that not much light is scattered directly upwards. This can be understood by noting that the incident field is dominated by its y component. The average total field $\mathbf{E}$ over a ridge is therefore mainly oriented along the y axis. It follows from the form of the Green's tensor $\mathbf{G}$ and Eq. (1) that for a field inside the ridge oriented along the y axis there will be no scattering in the direction of the y axis. This is similar to the case of a dipole (antenna) not emitting light in the direction of the polarization of the dipole. The effect is also seen in the

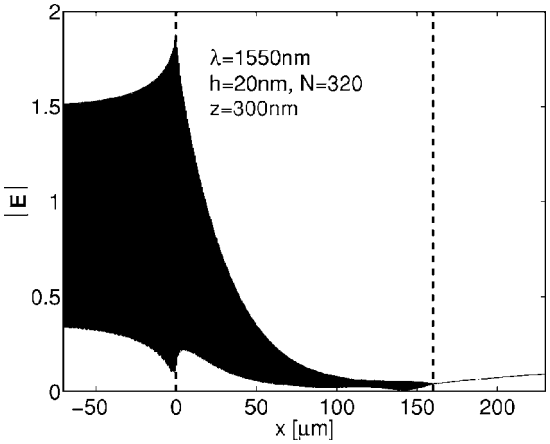

FIG. 6. Electric field magnitude versus position along a LRSPP grating with 320 ridges of height 20 nm. The fixed height $y=300$ nm above the gold film is considered. The wavelength is $\lambda=1550$ nm (in the bandgap).

case of scattering of a *p*-polarized plane wave incident on, e.g., a planar interface between two dielectric media. At the Brewster angle there is no reflection, which is due to the orientation of the electric field in the transmitting medium coinciding with the direction that the reflected wave must propagate.

From Fig. 5 it is not so easy to see the exponential field decay right at the surface for the wavelength in the band gap, which is in part because of a gray scale that enhances very small field magnitudes. Therefore we have in Fig. 6 plotted the electric field magnitude at the constant height above the gold film $y=300$ nm for the wavelength 1550 nm along the grating. Here the inhibition of propagation of the LRSPP is easily seen from the decay of the field magnitude envelope with x into the grating (the black filled regions contain very rapid oscillations in field magnitude with x). The small increase of the field magnitude for $x>160$ μm is due to diffraction.

We will finish this section by comparing theoretical results with a few experimental results, and show that the theoretically predicted effects are also seen in experimental measurements. In previous work[14] a comparison between theory and experiment was made for the case of ridge height 10 nm. In Figs. 7 and 8 we present both theoretical and experimental results of transmission and reflection for ridge heights ranging from 5 to 30 nm for a grating with 160 periodically placed gold ridges on each side of a 15 nm gold film (similar to the gratings described above). The experimental samples, the fabrication, and the measurements were similar to Ref. 14 except for the differences in ridge height. Notice that the reflection peak (Fig. 7) increases in width with ridge height h although the effect is less pronounced in the experiment. The short-wavelength edge of the band gap stays at approximately the same wavelength, whereas the long-wavelength band-gap edge shifts to longer wavelengths with h. This has also been observed theoretically for 2D arrays of surface scatterers.[22,24] In both theory and experiment it is seen that when we go from $h=20$ nm to $h=30$ nm the maximum reflection decreases (which we know is a consequence of out-

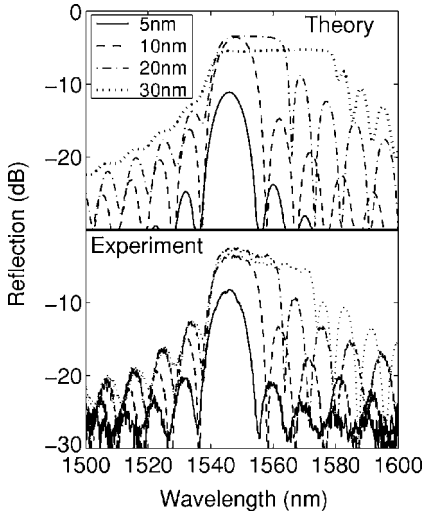

FIG. 7. Theoretical and experimental reflection spectra for LRSPP gratings with $N=160$ ridges for the ridge heights $h=5$, 10, 20, and 30 nm.

of-plane scattering in the theoretical calculation). The transmission curves (Fig. 8) show that also in the experiments higher transmission is observed on the long-wavelength side of the band gap compared to wavelengths shorter than the band gap. For all ridge heights considered, the band gap is easily identified from Fig. 7 as the range of the reflection peak. However, for the ridge height $h=30$ nm it has become more difficult to identify the band gap from transmission curves because the transmission on the short-wavelength side of the band gap can be comparable to or even smaller than the transmission in the band-gap range of wavelengths. For large ridge heights the transmission spectra become considerably more complicated than having just a dip for a band-gap range of wavelengths because coupling in and out of the grating, out-of-plane scattering, and absorption can result in very low transmission also for wavelengths well outside the band gap. This has also been observed theoretically for 2D SPP gratings.[24]

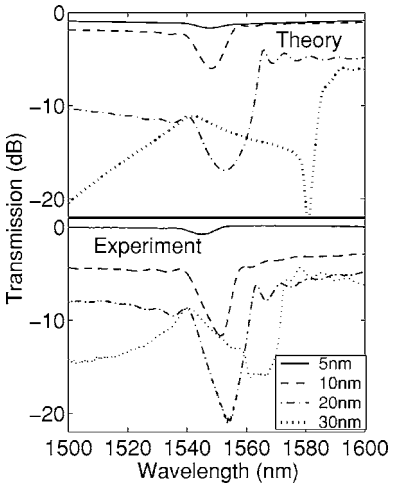

FIG. 8. Theoretical and experimental transmission spectra for LRSPP gratings with $N=160$ ridges for the ridge heights $h=5$, 10, 20, and 30 nm.

When comparing the theoretical and experimental curves for reflection (Fig. 7) we notice that the theoretical width of the band gap is slightly larger compared to the experimental observation. This might be a consequence of surface roughness in the experimental structures compared to the rectangular structure used in the calculation. Such imperfections in a grating structure would lead to a reduction in the width of the band gap. Concerning the theoretical and experimental transmission curves (Fig. 8) for the height 30 nm there are several qualitative similarities. First of all there is an increase in transmission with wavelength up to the wavelength 1540 nm. Above this wavelength the transmission decreases with wavelength until we reach the upper-wavelength band-gap edge (this edge can be identified from Fig. 7). At this wavelength, a sharp increase in transmission occurs after which the transmission for the rest of the spectrum remains at a value being significantly higher than any previous value for the transmission. Note that, as was the case for the reflection data, the upper-wavelength band-gap edge is shifted. Apart from this shift there is overall agreement between the main features of the theoretical and experimental curves.

IV. OPTICAL PROPERTIES OF SURFACE PLASMON POLARITON GRATINGS

The calculations in this section are similar to those in Sec. III with the exception that the structures considered here have an infinitely thick metal film ($d=\infty$). In this case a single metal-dielectric interface supports the surface waves known as surface plasmon polaritons (SPPs). We no longer refer to these waves that propagate along a single metal-dielectric interface as long-range waves, since the propagation length is significantly shorter due to increased ohmic losses related to absorption by the metal compared to the case of a thin gold film. The SPPs of a metal-dielectric interface are, however, more strongly bound than the LRSPPs of a thin metal film. For more strongly bound surface waves we may expect that the scattering from a single ridge will be more efficiently channeled into surface waves, such that the fraction of scattered light going into surface waves is larger compared to the total scattering including out-of-plane propagating waves.[37] As a result of having more strongly bound waves ridges of the same size will cover a larger fraction of the power cross section of the surface waves, and consequently we may expect the total scattering from a single ridge, including out-of-plane scattering, to be significantly larger. In this section we will investigate how the optical properties of SPP gratings are different compared to LRSPP gratings due to the increased propagation loss and stronger mode confinement.

The mode index for the SPP wave $\kappa_x/k_0=n_{\mathrm{SPP}}$ is 1.562 for the wavelength 1550 nm, which for very weak gratings leads to a band gap at wavelengths $\lambda\approx 2\Lambda n_{\mathrm{SPP}}=1562$ nm. Calculations of the optical properties for SPP gratings with ridge height $h=10$ nm and number of ridges $N=40$ and 160, respectively, are shown in Fig. 9. It is interesting that it is possible to achieve more than 40% peak reflection with only $N=40$ ridges. In order to achieve a similar reflection with the LRSPP gratings ($h=10$ nm) we will need 160 ridges. The

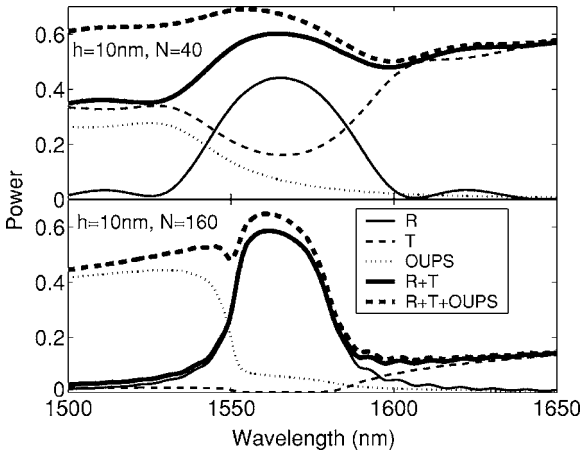

FIG. 9. Reflection (R), transmission (T), and out-of-plane scattering (OUPS) for SPP gratings with $N=40$ and 160 gold ridges of height $h=10$ nm.

loss due to absorption for SPP gratings ($1-R-T-\mathrm{OUPS}$) is, however, also 3–4 times larger depending on the wavelength. For the SPP grating with 160 ridges the peak reflection may approach 60%. For wavelengths longer than the band gap, the transmission is here below 20%, which is mainly due to an absorption of more than 80%. For wavelengths shorter than the band gap, the grating scatters efficiently out of the plane such that the loss due to OUPS is approximately 40%, and still more than 50% is lost due to absorption. If we increase the length of the grating further we do not obtain any significant improvement of the peak reflection. The peak reflection obtained with long LRSPP gratings with same ridge height ($h=10$ nm) and $N=320$ is higher than the maximum achievable reflection for the SPP grating. We may conclude that short SPP gratings will reflect more efficiently than short LRSPP gratings. However, the maximum achievable reflection will be higher when using long LRSPP gratings due to the smaller OUPS from the grating facets and the smaller absorption losses.

In Fig. 10 we consider SPP gratings with ridge height $h=20$ nm and the lengths $N=40$ and 160. Here the reflection with 40 ridges and 160 ridges is approximately 60% in both cases, such that a reflection better than 60% is not possible. The only effect of increasing the length beyond 40 periods is an increased absorption loss. We notice here that the smaller ridges ($h=10$ nm) did not make it possible to obtain any significantly larger reflection than what was possible with the larger ridges ($h=20$ nm) since it saturates at approximately 60%. This was different for the LRSPP gratings where a higher peak reflection was possible when using small ridges ($h=10$ nm) and long gratings ($N=320$) compared to using larger ridges (e.g., $h=20$ nm). The reason why higher reflection is not achieved here with the small ridges is the higher propagation loss related to absorption by the gold, which makes long gratings less attractive due to the associated long propagation distances in the grating with associated large absorption losses.

V. CONCLUSION

Optical properties of ridge gratings for LRSPPs have been studied theoretically by making use of the Lippmann-

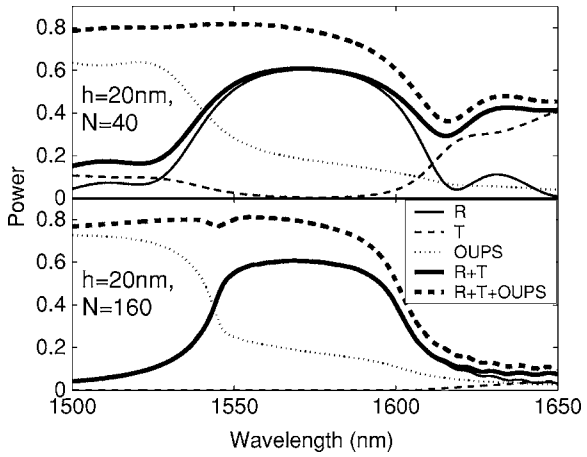

FIG. 10. Reflection (R), transmission (T), and out-of-plane scattering (OUPS) for SPP gratings with $N=40$ and 160 gold ridges of height $h=20$ nm.

Schwinger integral equation method, paying special attention to the process of OUPS. We considered the configuration with LRSPPs that propagate along a gold film embedded in dielectric and interact with a grating (designed for the BG wavelength of ~1550 nm) consisting of an array of gold ridges on each side of the film. The OUPS was found to be noticeably stronger for wavelengths shorter than the BG wavelength as compared to that for longer wavelengths, with the difference increasing with the grating length. The asymmetry in the OUPS with respect to the BG wavelength accounts for the fact that the transmission through LRSPP gratings is higher for wavelengths longer than the BG wavelength as compared to shorter wavelengths.[14,15] This asymmetry is related to the occurrence of out-of-plane LRSPP diffraction by the grating for wavelengths shorter than the BG wavelength. Note that, for all wavelengths, part of the OUPS loss takes place at the grating facets during coupling in and out of the grating of the LRSPP. Our calculations have also shown that the absorption loss decreases for wavelengths within the BG due to shorter LRSPP penetration in the grating and, consequently, smaller overlap between the field and the gold ridges. The largest reflection was found when using smaller ridges and longer gratings rather than gratings with larger ridges, since this reduces the OUPS related to the LRSPP coupling in and out of the grating. We have concluded, therefore, that the maximum peak reflection that can be achieved is ultimately limited by the (inherent) LSRPP propagation loss related to absorption by the film.

Field magnitude calculations were presented illustrating the OUPS for three different wavelengths being shorter, within, and longer than the BG. In the latter two cases, the OUPS was seen to originate mainly from the first facet of the grating, whereas, in the first case, it was observed that OUPS originated to a large extent from the interior of the grating region, as the grating efficiently couples to out-of-plane propagating waves.

Experimental measurements being in qualitative agreement with the theoretical calculations showed that, for LRSPP gratings with 160 ridges, the reflection peak decreases as the height of the ridges increase above a threshold (~20 nm). This is a direct consequence of the increase in the OUPS from the grating facets for larger ridges. The measured transmission spectra also exhibited asymmetry with respect to the BG wavelength, i.e., higher transmission was observed for wavelengths longer than the BG wavelength, a remarkable feature which has been established and accounted for in our theoretical analysis.

Finally, for SPP ridge gratings, corresponding to the case of a very thick gold film, it was found that longer gratings with smaller ridges (10 nm high) did not result in a higher SPP reflectivity as compared to that from shorter gratings with larger ridges (20 nm high). Contrary to the case of LRSPP gratings, it is, therefore, less attractive to use long (SPP) gratings due to higher propagation loss and stronger confinement of SPPs in comparison with LRSPPs.

Note added. When the manuscript was prepared for the submission we have learned of a paper by Sánchez-Gil and Maradudin[38] dealing with SPP gratings made of Gaussian shaped ridges, though neglecting the radiation absorption. The authors have calculated transmission and reflection spectra that are quite similar to those presented here [cf. Figs. 9 and 10 from this paper and Fig. 2 of Ref. 38] and also remarked on the increase of the OUPS for larger ridges.

ACKNOWLEDGMENTS

Part of the work was carried out while the authors were employed with Micro Managed Photons A/S. Kristjan Leosson and Thomas Nikolajsen are acknowledged for the fabrication and part of the characterization of the experimental samples considered in Figs. 7 and 8.

*Corresponding author; FAX: (+45) 98156502; Email address: ts@physics.aau.dk

[1] H. Raether, *Surface Plasmons* (Springer, Berlin, 1988).
[2] D. Sarid, Phys. Rev. Lett. **47**, 1927 (1981).
[3] J. J. Burke, G. I. Stegeman, and T. Tamir, Phys. Rev. B **33**, 5186 (1986).
[4] P. Berini, Phys. Rev. B **61**, 10484 (2000).
[5] A. Boltasseva, T. Nikolajsen, K. Leosson, K. Kjaer, M. S. Larsen, and S. I. Bozhevolnyi, J. Lightwave Technol. **23**, 413 (2005).
[6] S. J. Al-Bader, IEEE J. Quantum Electron. **40**, 325 (2004).
[7] W. L. Barnes, A. Dereux, and T. W. Ebbesen, Nature **424**, 824 (2003).
[8] S. I. Bozhevolnyi, J. Erland, K. Leosson, P. M. W. Skovgaard, and J. M. Hvam, Phys. Rev. Lett. **86**, 3008 (2001).
[9] S. I. Bozhevolnyi, V. S. Volkov, K. Leosson, and J. Erland, Opt. Lett. **26**, 734 (2001).
[10] S. I. Bozhevolnyi, V. S. Volkov, K. Leosson, and A. Boltasseva, Appl. Phys. Lett. **79**, 1076 (2001).

[11] S. I. Bozhevolnyi, V. S. Volkov, and K. Leosson, Opt. Commun. **196**, 41 (2001).
[12] R. H. Ritchie, E. T. Arakawa, J. J. Cowan, and R. N. Hamm, Phys. Rev. Lett. **21**, 1530 (1968).
[13] S. C. Kitson, W. L. Barnes, and J. R. Sambles, Phys. Rev. Lett. **77**, 2670 (1996).
[14] S. I. Bozhevolnyi, A. Boltasseva, T. Søndergaard, T. Nikolajsen, and K. Leosson, Opt. Commun. **250**, 328 (2005).
[15] A. Boltasseva, S. I. Bozhevolnyi, T. Søndergaard, T. Nikolajsen, and K. Leosson, Opt. Express **13**, 4237 (2005).
[16] S. Jetté-Charbonneau, R. Charbonneau, N. Lahoud, G. Mattiuse, and P. Berini, Opt. Express **13**, 4674 (2005).
[17] H. Ditlbacher, J. R. Krenn, G. Schider, A. Leitner, and F. R. Aussenegg, Appl. Phys. Lett. **81**, 1762 (2002).
[18] A. Bouhelier, Th. Huser, J. M. Freyland, H. -J. Güntherodt, and D. W. Pohl, J. Microsc. **194**, 571 (1999).
[19] S. I. Bozhevolnyi and V. Volkov, Opt. Commun. **198**, 241 (2001).
[20] F. I. Baida, D. Van Labeke, Y. Pagani, B. Guizal, and M. Al Naboulsi, J. Microsc. **213**, 144 (2004).
[21] M. Kretschmann, Phys. Rev. B **68**, 125419 (2003).
[22] T. Søndergaard and S. I. Bozhevolnyi, Phys. Rev. B **67**, 165405 (2003).
[23] I. R. Hooper and J. R. Sambles, Phys. Rev. B **70**, 045421 (2004).
[24] T. Søndergaard and S. I. Bozhevolnyi, Phys. Rev. B **71**, 125429 (2005).
[25] J. A. Sánchez-Gil, Phys. Rev. B **53**, 10317 (1996).
[26] F. Pincemin, A. A. Maradudin, A. D. Boardman, and J. -J. Greffet, Phys. Rev. B **50**, 15261 (1994).
[27] J. A. Sánchez-Gil and A. A. Maradudin, Phys. Rev. B **60**, 8359 (1999).
[28] A. V. Shchegrov, I. V. Novikov, and A. A. Maradudin, Phys. Rev. Lett. **78**, 4269 (1997); *ibid.* **79**, 2597 (1997).
[29] J. D. Joannopoulos, R. D. Meade, and J. N. Winn, *Photonic Crystals: Molding the Flow of Light* (Princeton University Press, Princeton, NJ, 1995).
[30] J. Arentoft, T. Søndergaard, M. Kristensen, A. Boltasseva, M. Thorhauge, and L. Frandsen, Electron. Lett. **38**, 274 (2002).
[31] A. Talneau, L. le Gouezigou, N. Bouadma, M. Kafesaki, C. M. Soukoulis, and M. Agio, Appl. Phys. Lett. **80**, 547 (2002).
[32] W. Bogaerts, P. Bienstman, D. Taillaert, R. Baets, and D. De Zutter, IEEE Photon. Technol. Lett. **13**, 565 (2001).
[33] D. Gerace and L. C. Andreani, Phys. Rev. E **69**, 056603 (2004).
[34] L. Novotny, B. Hecht, and D. Pohl, J. Appl. Phys. **81**, 1798 (1997).
[35] E. Palik, *Handbook of Optical Constants of Solids* (Academic, San Diego, CA, 1985).
[36] Kazuo Ohtaka and Jun-ichi Inoue, Phys. Rev. B **70**, 035109 (2004).
[37] T. Søndergaard and S. I. Bozhevolnyi, Phys. Rev. B **69**, 045422 (2004).
[38] J. A. Sánchez-Gil and A. A. Maradudin, Appl. Phys. Lett. **86**, 251106 (2005).